EFFECT OF STARTING GRAIN SIZE ON AS-DEFORMED MICROSTRUCTURE IN HIGH TEMPERATURE DEFORMATION OF ALLOY 718

D. Zhao and P. K. Chaudhury

Concurrent Technologies Corporation
1450 Scalp Avenue
Johnstown, PA 15904

Abstract

Two 718 alloys with initial grain sizes of 23 and 54 μm were tested in compression over wide ranges of temperatures (850-1150 C) and strain rates (0.001-25 s^{-1}) to investigate the effect of initial grain size on the flow behavior and resulting microstructure. The flow behavior was similar in both alloys. Elongated deformed grains were observed in specimens tested at relatively low temperatures, and dynamic recrystallization occurred at high temperatures. Percentages of dynamic recrystallization were measured for partially recrystallized conditions, and the recrystallized grain sizes were compared for the two alloys in completely recrystallized conditions. Despite the different initial grain size, the resulting grain size after dynamic recrystallization at high temperatures is comparable for the two alloys. However, the fine grain 718 alloy exhibited higher temperature for complete recrystallization at low strain rates. Processing conditions to produce uniform fine microstructure are recommended.

This work was conducted by the National Center for Excellence in Metalworking Technology, operated by Concurrent Technologies Corporation, under contract to the U.S. Navy as part of the U.S. Navy Manufacturing Technology Program.

Superalloys 718, 625, 706 and Various Derivatives
Edited by E.A. Loria
The Minerals, Metals & Materials Society, 1994

Introduction

Alloy 718 is one of the most important nickel-base superalloys, and currently accounts for 45 percent of wrought nickel-base alloy production [1]. Although this alloy has excellent workability and mechanical properties, more demanding property requirements make it necessary to control every step of processing [1], which includes thermomechanical processing. Over the past few years, several authors have studied this subject [2-5] in order to obtain optimum processing conditions that result in most favorable mechanical and microstructural properties in products. In high temperature deformation of alloy 718, the major event is dynamic recrystallization (DRX) that provides fine microstructures in finished products. The DRX process is affected by processing condition which determines the energy input into the material and the size, distribution, and stability of precipitates which interact with nucleation and growth of grains. It is generally believed that the initial grain size does not affect the recrystallized grain size as long as the DRX is complete. However, the initial grain size, in combination with the precipitate size and distribution, can determine the recrystallization mechanism, thereby dictating the DRX start and complete temperature, percent DRX, and corresponding flow behavior.

In this investigation, two 718 alloys with different initial grain sizes were tested in compression over wide ranges of temperatures and strain rates. Flow curves at test conditions were determined, and post-deformation microstructures were characterized. The results from this investigation are essential for process design in terms of obtaining desired microstructure through high temperature deformation processing.

Material and Experimental

Commercially available 718 wrought bars in the solutionized and aged condition were used in this investigation. The two initial grain sizes were 23 and 54 μm. Typical microstructures of the as-received materials are shown in Figure 1. They consist of equiaxed grains with some twins. Two groups of precipitates are present: (a) large niobium and titanium carbonitrides, and (b) fine γ' ($Ni_3(Al, Ti)$) which is the hardening phase in this alloy.

Cylindrical compression specimens with a diameter of 12.7 mm and a height of 15.9 mm were machined from the as-received bars. Isothermal compression tests were conducted in vacuum on a high speed servohydraulic MTS machine at temperatures 982, 1010, 1038, 1079, and 1149 C and strain rates 0.01, 0.14, 1.84, 5, and 25 s^{-1} to a true strain of 0.6 for the alloy with small (23 μm) initial grain size, and at temperatures 850, 900, 950, 1000, 1050, 1100, and 1150 C and strain rates 0.001, 0.01, 0.05, 0.1, 0.5, 1, 5, and 20 s^{-1} to a true strain of 0.8 for the alloy with large (54μm) initial gain size.

Prior to compression, each specimen was soaked at the test temperature for 10 minutes to obtain uniform temperature distribution. Load and stroke data from the tests were acquired by a computer and later converted to true stress-true strain curves. Immediately after the compression test, the specimens were quenched with forced helium gas to retain the deformed microstructure. The initial cooling rate (from the test temperature to 600 C) was measured using a thermocouple inserted in the specimens, and varied between 300-500 C/min, depending on the test temperature. The deformed specimens were sectioned through the longitudinal axis and metallographically prepared. The microstructures were examined utilizing an Olympus optical microscope equipped with a Leco image analyzer, and the average grain size was measured using intercept method. The photomicrographs presented were taken from the center of the longitudinal sections.

Results and Discussion

The true stress-true strain curves for all test conditions with selected as-deformed microstructures of the two 718 alloys were reported elsewhere [6-7]. There are basically three types of flow curves for the large grain alloy (54 μm) after the initial work hardening: 1) flow softening, 2) steady state flow, and 3) flow softening followed by steady state flow and subsequent flow hardening. Occurrence of these three types of flow are shown schematically in

terms of temperature and strain rate in Figure 2. Work hardening followed by continuous softening occurred at high strain rates (Figure 3), and the regime moved to higher strain rate as temperature was increased. The primary reason for this continuous softening was deformation heating. At high temperatures, deformation heating became only significant at very high strain rates. As a result, flow softening was observed at 900 C and a strain rate of 0.5 s^{-1}, and only at a strain rate of 20 s^{-1} when temperature increased to 1150 C. DRX also contributed to the softening. Both partial and complete DRX was observed at high strain rates depending on the

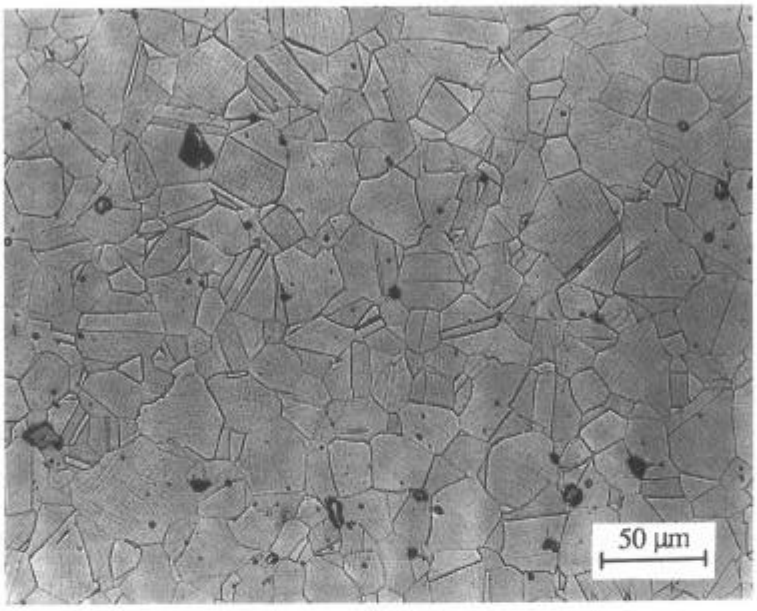

(a)

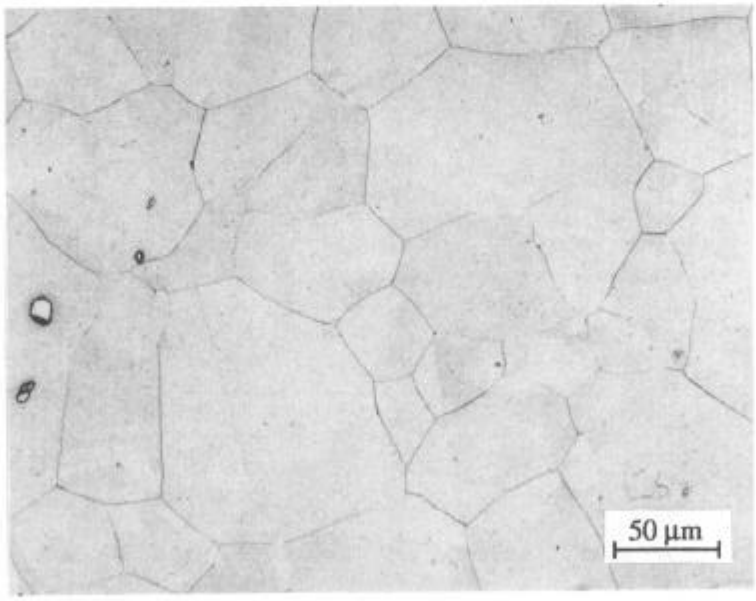

(b)

Figure 1 - As-received microstructures for 718 alloys, average grain size (a) 23 µm, and (b) 54µm.

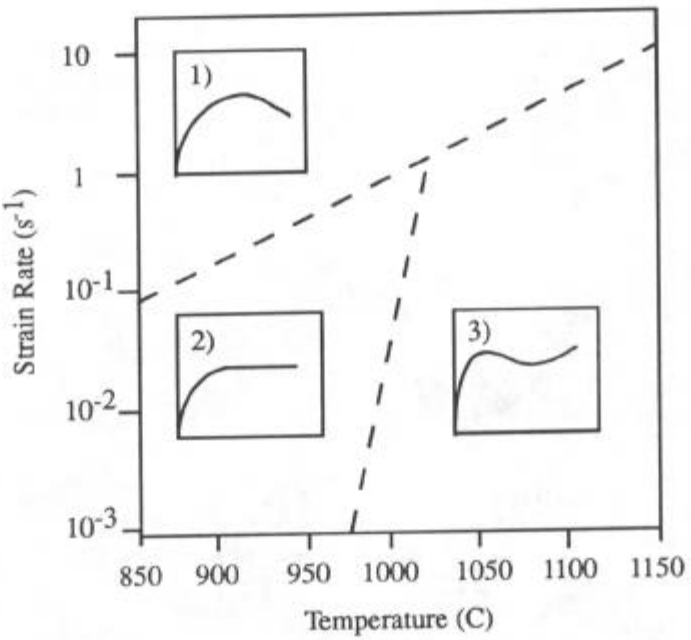

Figure 2 - Schematic of the three types of flow behavior as a function of temperature and strain rate.

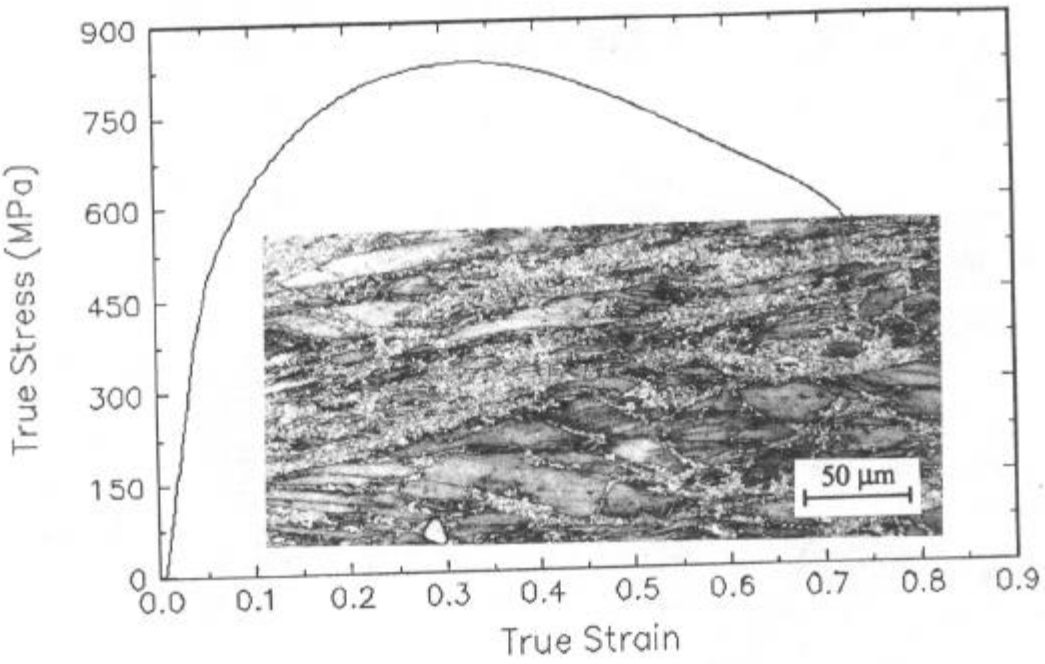

Figure 3 - Flow curve and as-deformed microstructure of the 718 alloy with initial grain size 54 µm, 850 C and 20 s^{-1}.

deformation temperature. The second flow behavior was observed at low temperatures and low strain rates. In this case, dynamic recovery (DRV) occurred at lower temperatures and DRX at higher temperatures. The work hardening and the softening caused by these restoration processes were balanced and resulted in constant flow stress after the initial work hardening; see

Figure 4. There were very small amounts of hardening or softening in some cases, depending on the temperature and the strain rate. The third flow behavior was observed at relatively high temperatures and low strain rates, where complete DRX took place. The DRX was complete at small strains causing the initial peak on flow curves. Depending on the strain rate, continued straining after DRX increases dislocation density and also provides time for grain growth to increase high temperature creep strength of the material, Figure 5. At very high temperatures and lower strain rates, grain growth becomes predominant, while at lower temperatures and higher strain rates work hardening of newly recrystallized grains contribute significantly.

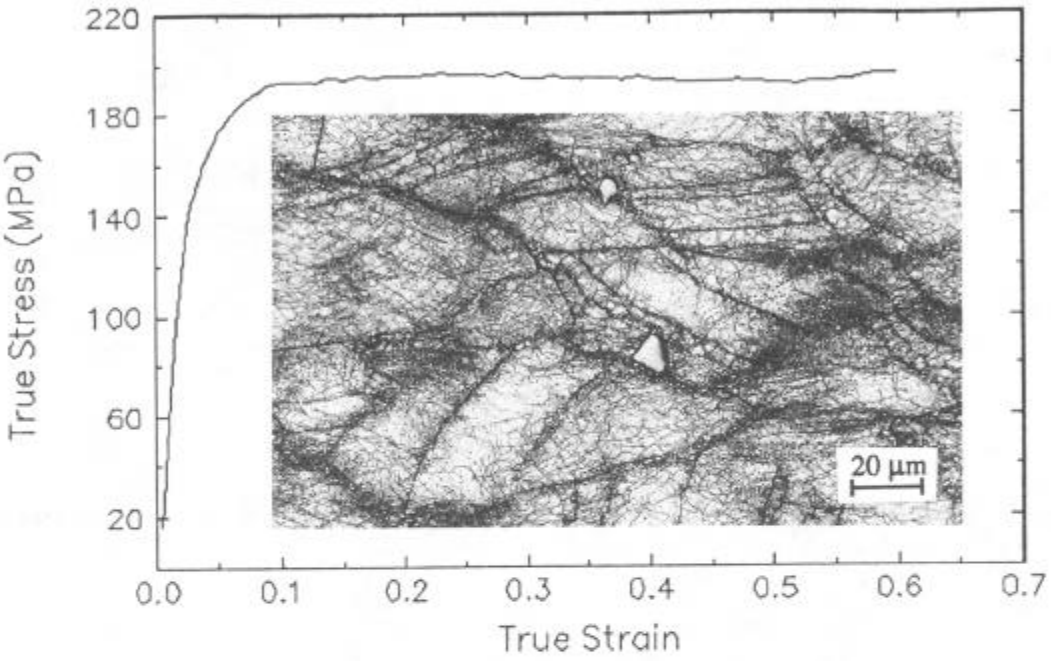

Figure 4 - Flow curve and as-deformed microstructure of the 718 alloy with initial grain size 54 µm, 900 C and 0.001 s^{-1}.

The small grain (23 µm) alloy showed similar flow behavior to that of the large grain alloy. However, the difference in grain size affected the DRX temperature; the smaller grain size resulted in different temperature and strain rate regimes for the three flow behaviors.

Figures 6 and 7 show the percentage of DRX as a function of temperature and strain rate for the large and small grain alloys respectively. Dynamic recrystallization initiated at a temperature of 850 C for the large grain alloy, Figure 6. At low temperatures, the amount of mechanical energy input and deformation heating had predominant effect on the recrystallization behavior; the amount of recrystallization increased as strain rate increased. At 850 C the maximum percentage of recrystallization was approximately 40% at the highest strain rate 20 s^{-1}. With increase in temperature, the effect of time at test temperature started to play an important role in the recrystallization process. This resulted in the minimum percent recrystallization at intermediate strain rates where neither the deformation heating is significant, nor the test time is long enough for recrystallization. There were evidence that considerable static recrystallization can occur at 924 C and above [9], which explains the higher percentage of recrystallization with longer exposure time at low strain rates. However, if the temperature is too low, staying longer at the temperature would not help recrystallization. Large grain alloy exhibited complete recrystallization at 1000 C and all strain rates, while the small grain alloy was partially recrystallized at 1010 C and 0.01 s^{-1}. For small grain alloy at temperatures 982 and 1010 C, which are comparable to the temperature of 1000 C for the large grain alloy, the percentage of recrystallization is much lower at intermediate strain rate such as 0.01 s^{-1}, Figure 7 However, at high strain rates, it became comparable to that of the large grain alloy. The data by Howsen and

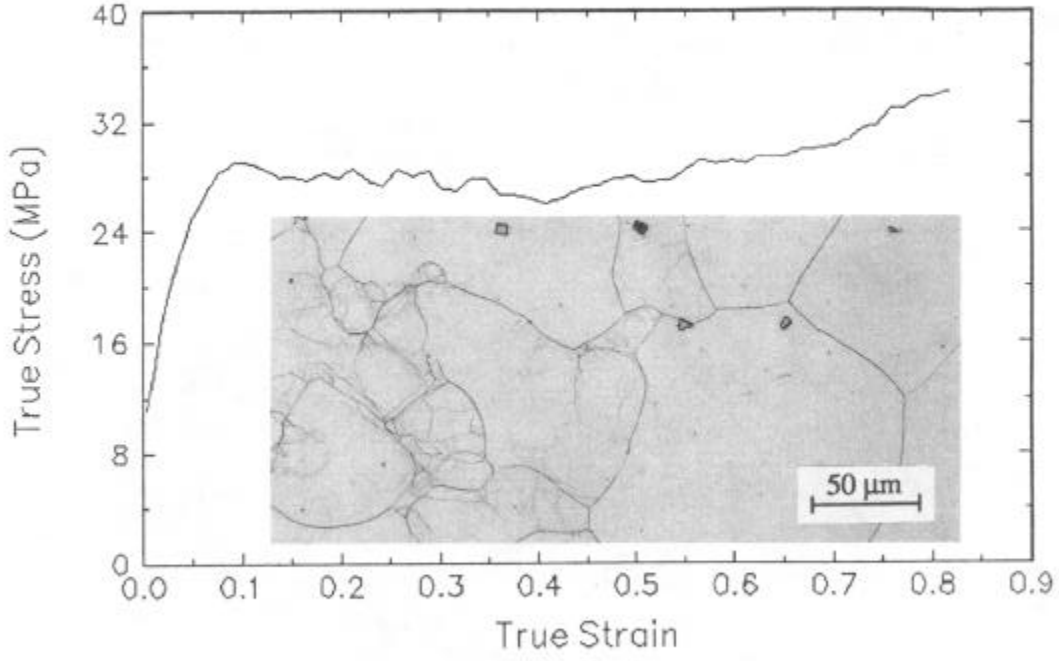

Figure 5 - Flow curve and as-deformed microstructure of the 718 alloy with initial grain size 54 µm, 1150 C and 0.001 s^{-1}.

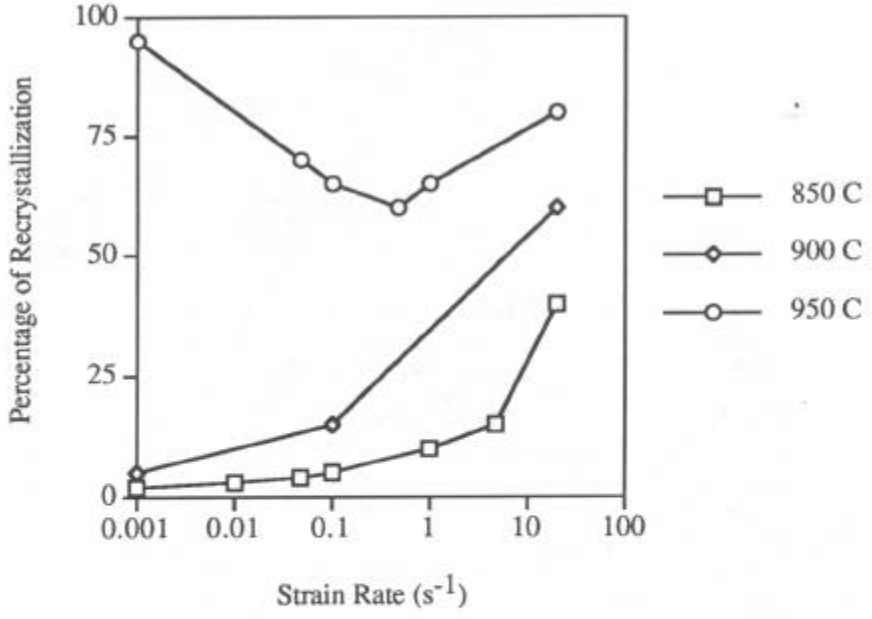

Figure 6 - Percentage of recrystallization as a function of temperature and strain rate for the 718 alloy with initial grain size 54 µm.

Couts [5] on fine grain (average 34 µm) was also plotted on the graph, which shows complete recrystallization at 982 C and above and strain rate of 0.001 s^{-1}. The results indicate that the

recrystallization of small grain alloy is more difficult than that of large grain alloy. The possible explanation is that small grain alloy can accommodate strain by grain boundary sliding more easily than the large grain alloy, and result in lower stored strain energy that facilitates recrystallization.

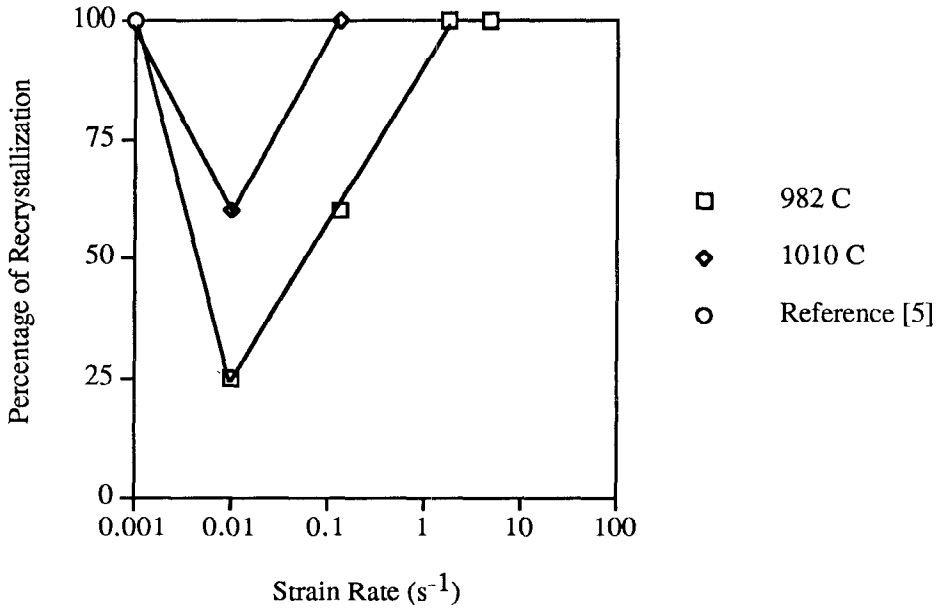

Figure 7 - Percentage of recrystallization as a function of temperature and strain rate for the 718 alloy with initial grain size 23 μm.

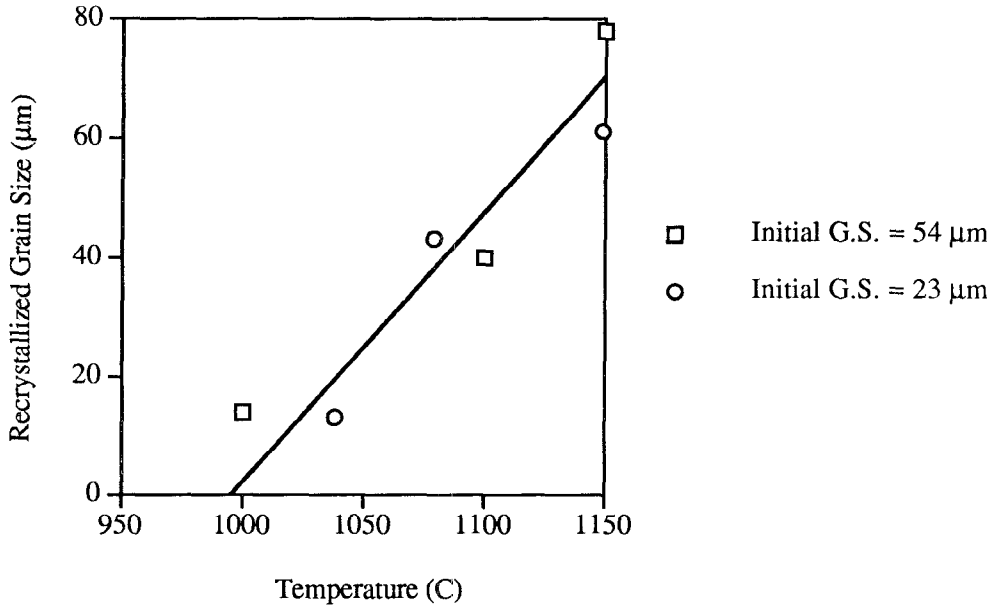

Figure 8 - Average grain size of the recrystallized grains as a function of temperature at strain rate of 0.01 s^{-1}.

The recrystallized grain sizes of the two alloys were compared in Figures 8 and 9. Figure 8 presents the recrystallized grain sizes of both alloys as a function of temperature at a strain rate of

0.01 s^{-1}, and Figure 9 shows the same as a function of strain rate at temperatures 1150 and 1149 C. The grain size is comparable for the two alloys for either of the conditions, which confirmed that dynamically recrystallized grain size is not a function of initial grain size. The grain size is close to a linear function of temperature, Figure 8, and an exponential function of log strain rate, Figure 9.

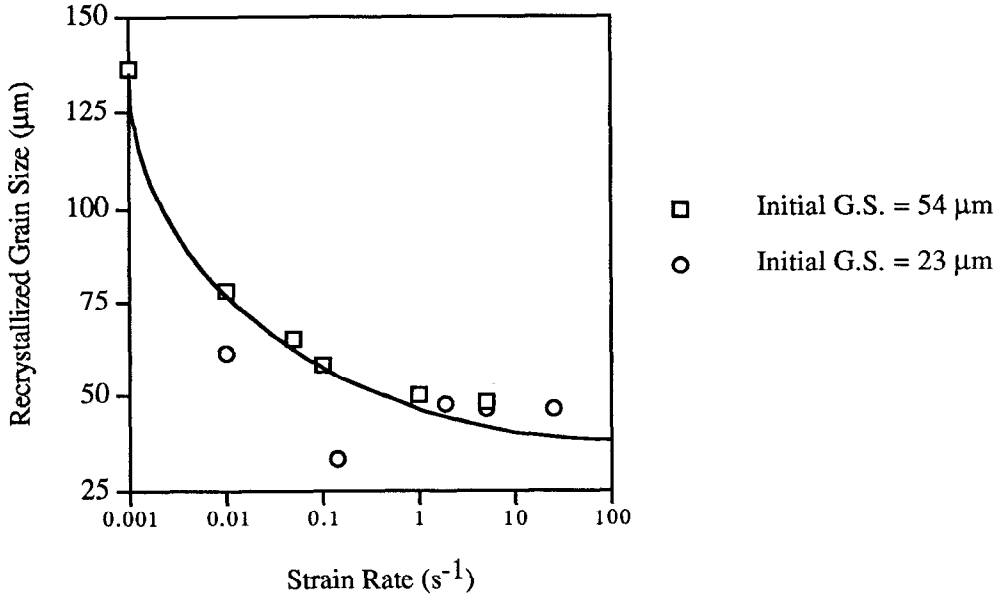

Figure 9 - Average grain size of the recrystallized grains as a function of strain rate at temperatures of 1150 and 1149 C.

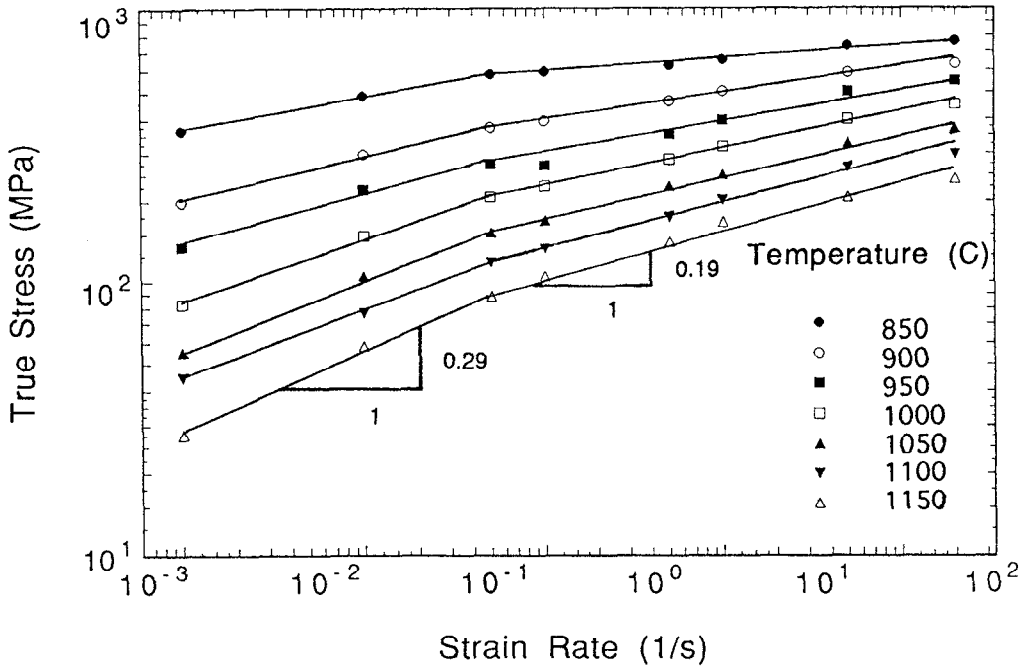

Figure 10 - Effect of strain rate on flow stress for the 718 alloy with initial grain size 54 μm at a true strain of 0.5.

The effect of strain rate on flow stress is shown in Figures 10 and 11 for the large grain alloy at a true strain of 0.5 and the small grain alloy at a true strain of 0.3, respectively. In both alloys, the strain rate sensitivity (slope of the plots), generally increased with increasing temperature and decreasing strain rate. Similar to alloy 625 [10], there was a transition of flow behavior as the strain rate sensitivity changed to a lower value with increase in strain rate. However, the strain rate sensitivity values and the transition strain rate differed for the two alloys. The large grain alloy exhibited a power law creep type transition from viscous slide ($m = 0.3$) to climb ($m = 0.2$) controlled deformation at $5x10^{-2}$ s^{-1}, while the small grain alloy exhibited power law breakdown type transition from climb ($m = 0.2$) controlled deformation to power law breakdown ($m < 0.2$) at higher strain rates (2 s^{-1}), both typical of fcc solid solution alloys [11-15].

The effect of temperature on flow stress for the large and small grain alloys are shown in Figures 12 and 13 respectively. The data basically fit a straight line except at high strain rates and low temperatures at which the deviation may be caused by deformation heating. There is no dramatic change in apparent activation energy of deformation, and is consistent with deformation characteristics of fcc solid solution alloys [11-15].

By considering both strain rate sensitivity and as-deformed microstructure, the recommended processing conditions for uniform deformation that result in fine microstructure are 1000 C at strain rates of 0.01 to 0.1 s^{-1} for the large grain alloy, and the same temperature at strain rates of 0.14 to 1.84 s^{-1} for the small grain alloy.

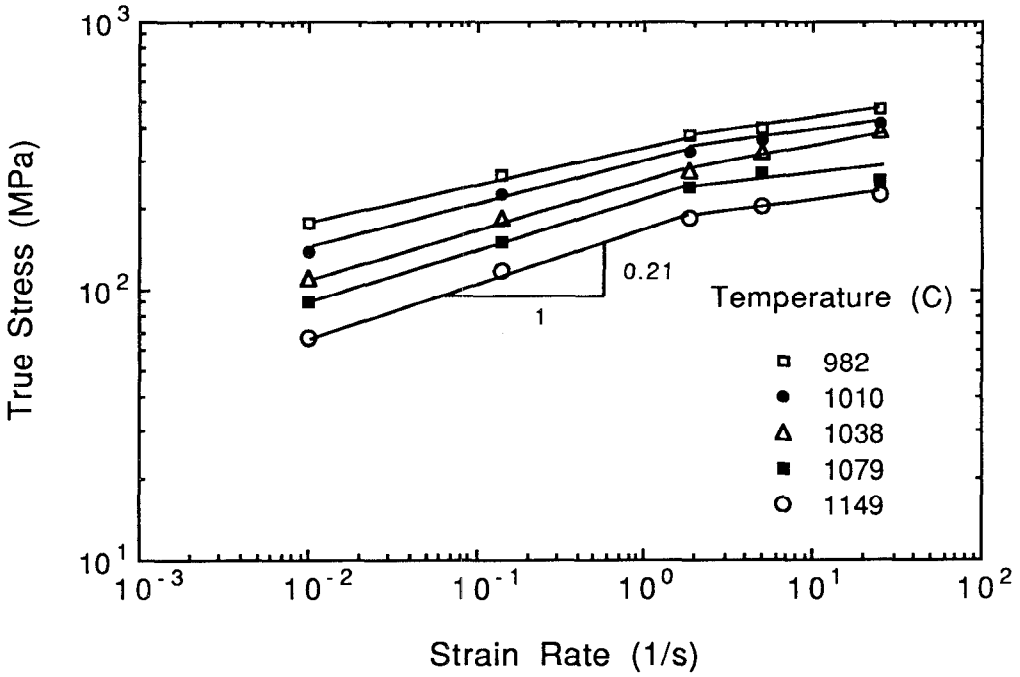

Figure 11 - Effect of strain rate on flow stress for the 718 alloy with initial grain size of 23 μm at a true strain of 0.3.

Summary and Conclusions

Effect of staring grain size on as-deformed microstructures was studied by conducting compression tests on two 718 alloys over a wide range of temperatures and strain rates. The following conclusions can be drawn.

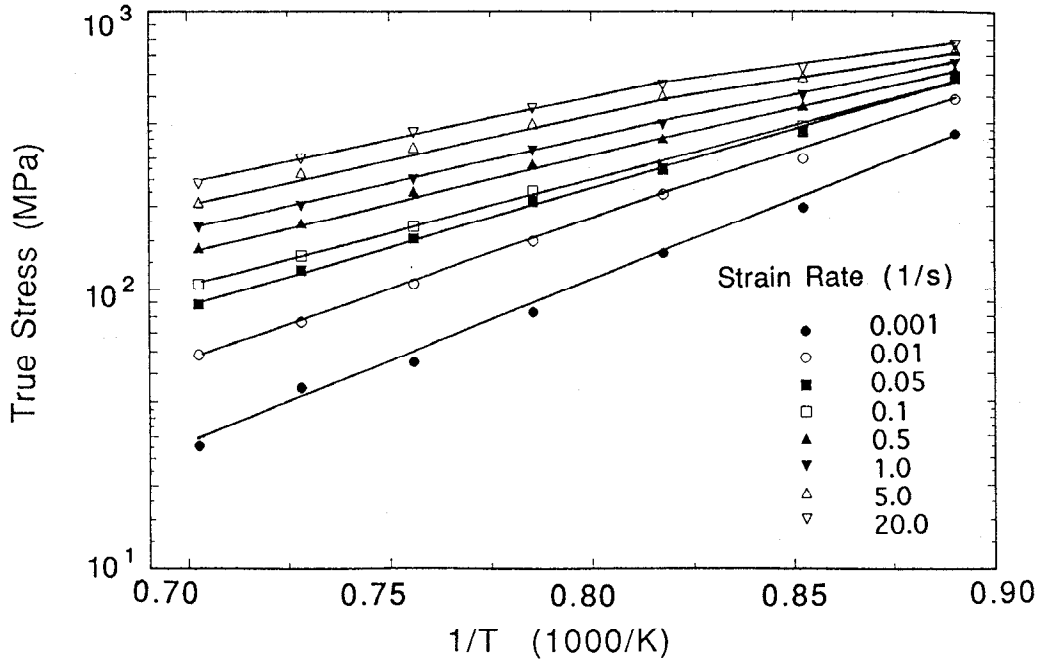

Figure 12 - Effect of temperature on flow stress for the 718 alloy with initial grain size 54 μm at a true strain of 0.5.

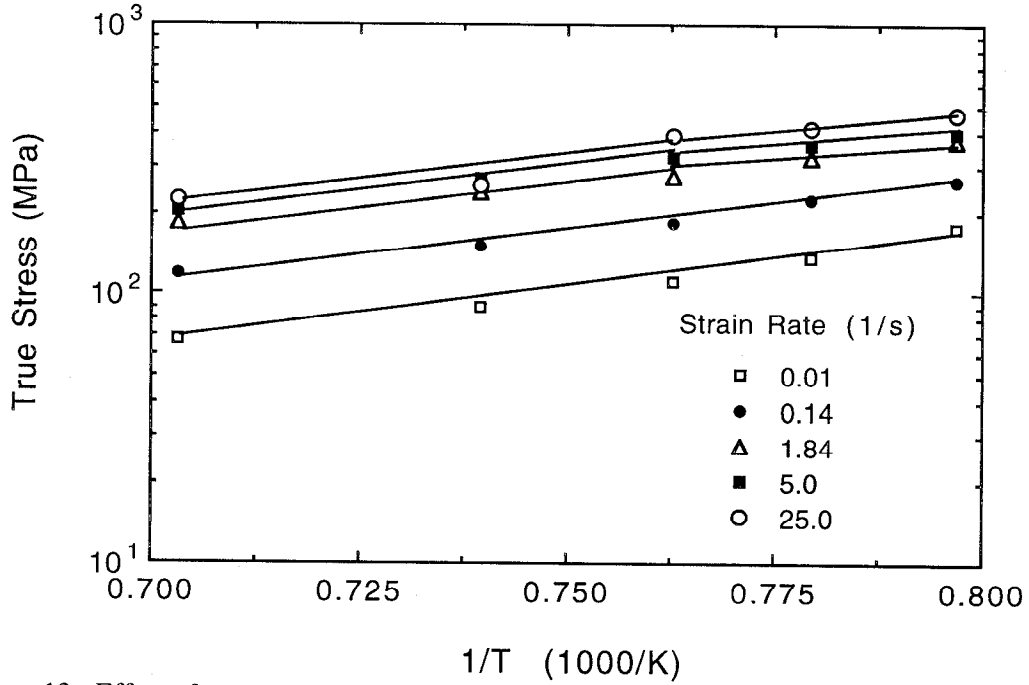

Figure 13 - Effect of temperature on flow stress for the 718 alloy with initial grain size of 23 μm at a true strain of 0.3.

1. Three types of flow curves were identified after initial work hardening: 1) flow softening, 2) steady state flow, and 3) flow softening followed by steady state flow and subsequent flow hardening. The contribution of softening were mainly from dynamic recrystallization, and deformation heating at high strain rates.

2. Percentage of dynamic recrystallization at a constant temperature is dependent on the initial grain size at intermediate strain rate, such as 0.01 s^{-1}. Smaller initial grain size resulted in lower percentage of dynamic recrystallization.

3. Initial grain size does not affect the recrystallized grain size in completely recrystallized conditions.

4. Recommended processing conditions for uniform deformation and fine microstructure: 1000 C and 0.01 to 0.1 s^{-1} for the alloy with initial grain size 54 μm, and 1000 C and 0.14 to 1.84 s^{-1} for the alloy with initial grain size of 23 μm.

References

1. E.A. Loria, JOM, June 1992, 33-36.

2. P.K. Chaudhury, D. Zhao, J.J. Valencia, and G.E. Holt, Concurrent Engineering Approach in Materials Processing, ed. S. N. Dwivedi, A. J. Paul, and F. R. Dax (Warrendale, PA: TMS, 1992), 81-92.

3. A. A. Guimaraes and J. J. Jonas, Metall. Trans. A, 12A (1981), 1655-1666.

4. T. E. Howson and W. H. Couts, Jr., Superalloys, Supercomposites and Superceramics (Academic Press, Inc., 1989), 183-214.

5. T. E. Howson and W. H. Couts, Jr., Superalloy 718-Metallurgy and Applications, ed. E. A. Loria (Warrendale, PA: TMS, 1989), 685-694.

6. Atlas of Formability Bulletin Inconel 718 (Johnstown, PA: National Center for Excellence in Metalworking Technology (NCEMT), 1992).

7. Atlas of Formability Bulletin Allvac 718 (Johnstown, PA: National Center for Excellence in Metalworking Technology (NCEMT), 1992).

8. S.L. Semiatin and J.J. Jonas, Formability & Workability of Metals (Metals Park, OH: ASM International, 1984), 43-148.

9. R.P. Singh, J.M. Hyzak, T.E. Howsen and R.R. Biederman, Superalloy 718, 625 and Various Derivatives, ed. E.A. Loria (Warrendale, PA: TMS, 1991), 205-215.

10. D. Zhao, P.K. Chaudhury, R.B. Frank, and L.A. Jackman, Superalloy 718, 625, 706 and Derivatives, ed. E.A. Loria (Warrendale, PA: TMS, 1994).

11. P.K. Chaudhury and F.A. Mohamed, Metall. Trans. A, 18A (1987), 2105-2114.

12. P.K. Chaudhury and F.A. Mohamed, Mat. Sci. Eng. A, 101 (1988), 13-23.

13 P. Yarani and T.G. Langdon, Acta Metall., 30 (1982), 2181-2196.

14. M.S. Soliman and F.D. Mohamed, Metall. Trans. A, 15A (1986), 1873-1906.

15. M.S. Soliman, Res. Mech., 21 (1987), 155-163.